Journal of
Composites Science

Article
Filling Time Reduction in Liquid Composite Molding Processes

Felice Rubino [1,*], Fausto Tucci [2], Vitantonio Esperto [2] and Pierpaolo Carlone [2]

[1] DIMME–Durability and Mechanical Integrity of Structural Materials, Escuela Superior de Ciencias Experimentales y Tecnología, Department of Chemical Universidad Rey Juan Carlos, C/Tulipán, 28933 Móstoles, Spain
[2] Department of Industrial Engineering, University of Salerno, Via Giovanni Paolo II, 132, 84084 Fisciano, Italy
* Correspondence: felice.rubino@urjc.es

Abstract: The quality of Liquid Composite Molding (LCM) manufactured components is strictly related to the fibrous preform impregnation. As Darcy's law suggests, the resin flow is influenced by the pressure gradient, geometrical features of the reinforcement, and resin viscosity. The former two parameters are dictated by the requirements of the component and other constraints; therefore, they are hardly modifiable during the process. Resin preheating increases its fluency, thus enhancing the impregnation and saturation flow, and reducing the mold filling time. In the present work, a microwave heating system has been integrated within a vacuum bag resin infusion process, to analyze the effect of the online preheating on the fiber impregnation. To monitor the resin flow a dielectric sensors-based system is used. Results from resin infusion tests conducted with and without the resin pre-heating were compared: the outcomes indicated an advance of approximately 190 s of the flow front when microwave heating is applied with respect to the unheated tests.

Keywords: liquid composite molding; microwave preheating; dielectric flow monitoring

check for updates

Citation: Rubino, F.; Tucci, F.; Esperto, V.; Carlone, P. Filling Time Reduction in Liquid Composite Molding Processes. *J. Compos. Sci.* **2022**, *6*, 222. https://doi.org/10.3390/jcs6080222

Academic Editor: Jinyang Xu

Received: 12 July 2022
Accepted: 2 August 2022
Published: 4 August 2022

1. Introduction

Liquid composite molding (LCM) processes, such as resin transfer molding (RTM) or Seemann composites resin infusion molding (SCRIMP) processes have been addressed by composite industries as a promising technology to manufacture polymeric matrix composites out-of-autoclave. Some of these processes are particularly interesting for the industry involved in the production of large-scale structures, even with complex shapes [1]. However, large scale diffusion of components depends on the possibility to lower the overall costs of the products and scale-up the technology to a mass production, always guaranteeing the quality of the manufactured composite structures [2].

In LCM processes, the final quality of the products is strictly connected to the impregnation and curing phases [3]. Dry spots or excess in resin, delamination or cracks, and residual stress are some of the most common flaws that can occur during the manufacturing compromising the performance and the integrity of the structure if the mentioned aspects are not carefully designed and monitored [4,5]. Impregnation defects can be related to the incompatibility of the two main phases involved. From this point of view, the binder plays a key role [6].

Sensing techniques have been developed to monitor both resin flow front progression and the cure degree in thermoset matrix composite manufacturing processes. They include, but are not limited to, the use of optical FBG sensors [7–9] pressure transducers [10], thermocouples [11–14], SMART weave sensor [15,16], electrical time domain reflectometry (ETDR) [15], ultrasonic, dielectric and piezoelectric sensors [17–22]. In their previous works, authors developed a sensing system based on dielectric analysis (DEA) to monitor the resin flow progression during the Resin Infusion process [19,20]. DEA relies on the measurement of the dielectric properties, i.e., permittivity and ionic conductivity of the test material: dielectric material is placed between electrodes forming a capacitor and an alternating electric field is applied across the plates, then permittivity, loss factor and ionic conductivity can be determined from the output current [23]. Dielectric sensors, consisting of parallel plates placed on both sides of a mold, were implemented in a lab-scale LCM apparatus and provide pieces of information on the resin arrival at the sensor position by detecting variation in the dielectric properties of the medium (glass fibers plus resin) [20,24]. Since the electrodes can be placed outside of the composite laminate, the sensing system is less invasive and does not affect either the integrity of the manufactured parts or the surface finishing of the part.

In addition, the parallel plate dielectric sensors are characterized by a higher scanning depth, which makes this design suitable also for thick composite [24,25]. The plane plates dielectric sensors require that the sensing areas of the electrodes must be parallel to each other, and the reciprocal distance must be known and kept constant during the entire infusion process. This limited the usage of these types of dielectric sensors only to specific classes of LCM processes using rigid molds, such as RTM, which ensures that these requirements are observed. LCM processes involving flexible upper mold, such as Vacuum Assisted Resin Infusion (VARI) or SCRIMP processes, were coupled only with co-planar dielectric sensors [16,26]. To the authors' best knowledge, no attempts have yet been made to apply parallel-plates dielectric sensors to monitor these processes.

In addition to the monitoring and the control of impregnation and curing phases to ensure the quality of the composite parts, the scale-up of the composite industry to a mass-production is also limited by the manufacturing time of a component, dictated by the time required to fully impregnate the fibrous reinforcement and the time to complete the curing of the resin. This is especially true in the case of big components, such as boat hulls (usually manufactured by the SCRIMP process), where the impregnation is particularly long and the curing of resin is deliberatively kept slow to avoid gelation prior to the complete wetting [27]. In this scenario, enhancing strategies of the resin flow through the fabric is of paramount relevance to achieve a uniform impregnation of the fibers and optimize the filling time, mitigating the manufacturing flaws and contributing to a reduction in the overall production time of a composite structure. Among the strategies investigated, the reduction in resin viscosity by means of mold temperature increases [28]; preform or resin preheating [28–31] can improve the flow through the preform and, thus, decrease the impregnation time. Dealing with thermosetting resin systems involves time-temperature constraints related to its reactivity and the consequent reduction in pot life. From this point of view, microwave-based heating systems guarantee a high efficiency thermal energy transfer. Reductions in filling time of about 13% and 25% have been obtained in the case of non-reactive and reactive systems, respectively, by optimizing the microwave heating apparatus [32–35].

Previous experiments have been dedicated to the study of the resin flow through a dry fibrous preform sealed between rigid molds [32–35]. In the present article, the author investigated the application of microwave preheating to the SCRIMP process to reduce the filling time. Parallel plate dielectric sensors were also implemented to monitor the resin flow. An ad-hoc system was developed to install the electrodes on the vacuum bag and ensure the correct alignment of the plates during the whole process.

2. Materials and Methods

The liquid composite molding (LCM) experimental was conducted based on the following preliminary requisite materials along with the ancillary materials. HexForce E-glass twill 2/2 fabric was used as reinforcing material. 12 layers of the glass fiber fabric were cut into rectangular plies with dimensions 300 mm × 240 mm. Main properties of the reinforcement are indicated in Table 1.

Table 1. Reinforcement properties.

Reinforcement	Glass Fiber (E-Glass)
Weave style for intended preform	Twill 2/2 fabric
Areal density	390 g/m^2
Fabric thickness	0.3 mm
Construction	90° warp/weft

Epoxy resin SX 10 was utilized upon the room temperature premixing with the Epoxy-based hardener in the mixing ratio of 100:26. The resin properties are mentioned in Table 2. Its rheological behavior measured by rheometry testing is depicted in Figure 1 and described by the following equation:

$$\eta = A_\eta \, exp\left(\frac{B_\eta}{R\,T} + C_\eta \alpha\right), \tag{1}$$

where the viscosity η depends on the pre-exponential term $A_\eta = 7.093 \times 10^{-8}$ [Pa·s], the calibration coefficients $B_\eta = 3.999 \left[\mathrm{J{\cdot}mol^{-1}}\right]$ and $C_\eta = 1.63$, the universal constant of gases $R = 8.314 \left[\mathrm{J\,K^{-1}{\cdot}mol^{-1}}\right]$, the temperature T expressed in Kelvin degrees, and the degree of cure of the resin system α.

Table 2. Resin matrix properties.

Matrix	Epoxy SX10 EVO
Viscosity at 25 °C	0.250~1.20 Pa·s
Gardner index	3
Density at 20 °C	1100 kg/m^3
Flash point	>100 °C

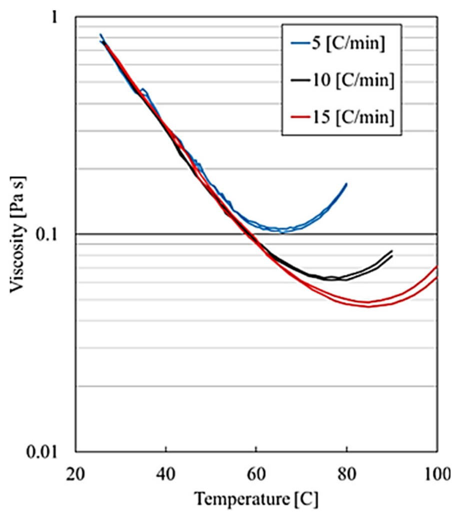

Figure 1. Viscosity of resin system as function of temperature and heating rate.

The vacuum bagging setup is shown in Figures 2 and 3, and it consists in the following steps:

1. Application of PVA release agent on the upper side of the mold;
2. Positioning of 12 sheets of glass fiber;
3. Positioning of peel ply and distribution media;
4. Positioning of the vacuum bag.

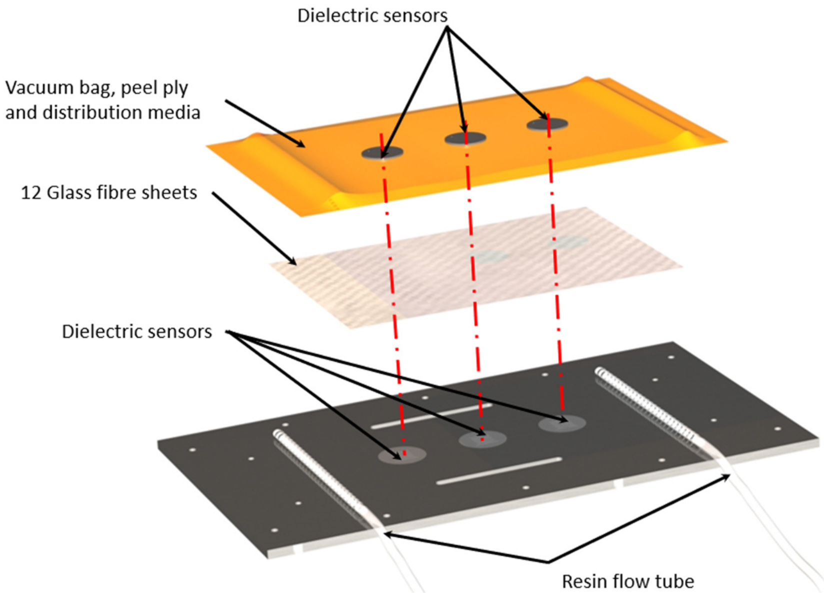

Figure 2. Vacuum bagging setup scheme.

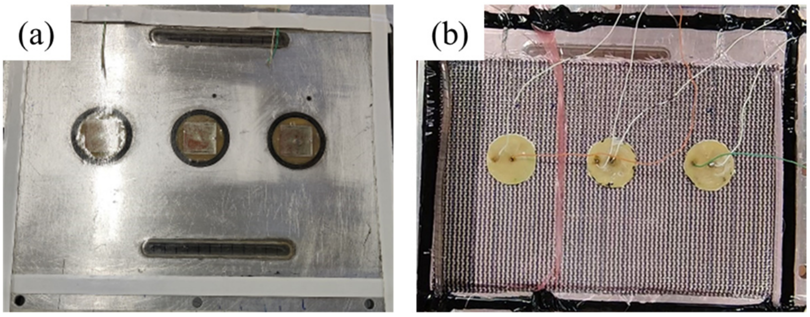

Figure 3. (**a**) Lower half-mold embedding the dielectric armatures. (**b**) Upper armatures mounted along with the soldered connecting wires over the vacuum bag during the resin flow progression.

The used ancillary materials, such as resin flow tubes and sealant tapes, were able to withstand high temperature. This selection was taken considering the temperature increase due to microwave preheating.

The lower armatures of the dielectric sensors are embedded in the rigid mold, as illustrated in Figures 2 and 3a. The armatures consist of square copper plates (25 $\times$ 25 mm^2) located at 60, 150, and 240 mm from the resin inlet, respectively. The three upper armatures of the capacitive sensors were fixed on the vacuum bag in correspondence to the lower ones. The eyelets milled in the rigid lower and sealed by transparent plastic allow to visually monitor the bottom-side flow. Two cameras were focused on the vacuum bag and on the eyelet during the entire test to monitor the position of the resin flow front.

Spiral wraps were inserted for the easy entry and exit of the resin under the vacuum bag. The vacuum bag encompassing the fibrous preform was sealed using the sealant tape avoiding any spot for external air insertion. The vacuum was induced by attaching the resin outlet tube to the vacuum pump. The resin inlet was clamped and negative air pressure of 0.9 bar was maintained to place the entire arrangement under vacuum conditions. Figure 4 shows the two schemes adopted to carry out the laboratory tests: the upper scheme represents the setup without microwave preheating; the lower is the setup involving the microwave preheating.

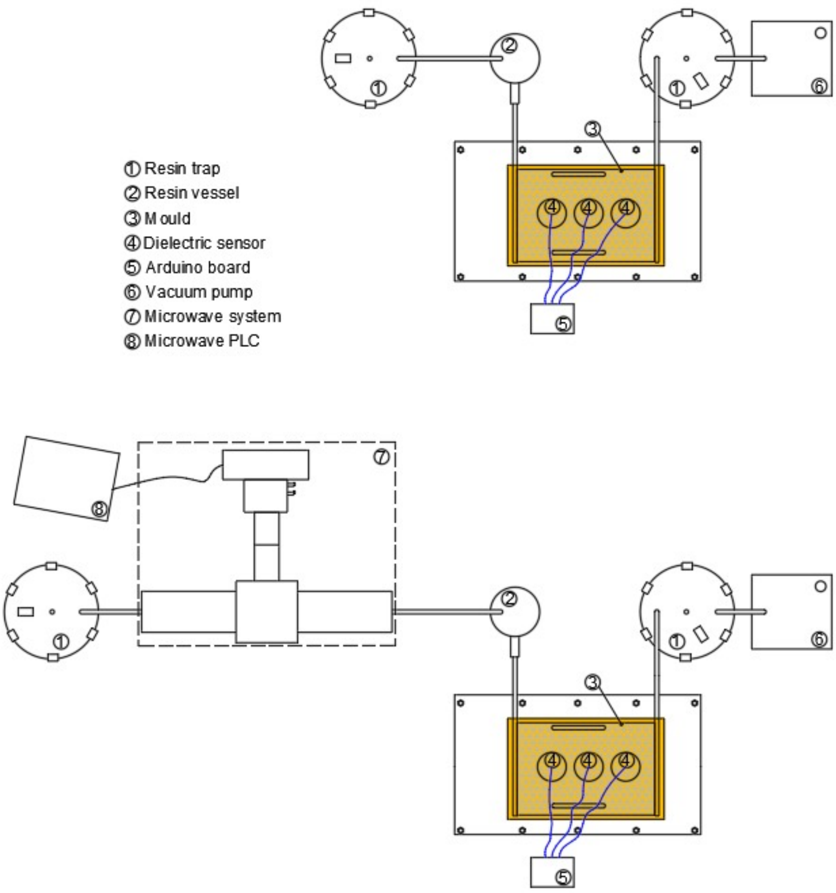

Figure 4. Schematic representation of the experimental setup of the resin infusion mold equipped with the dielectric and thermal acquiring system.

The microwave facility, depicted in Figure 4, consists of a 2 kW microwave generator, stainless steel waveguides, cylindrical resonance cavity, and ancillary tools. The choice of a microwave-based system to preheat the resin is based on the thermo-chemical and rheological behavior of the thermosets. Indeed, these polymeric systems are characterized by short pot-lives, which are further reduced when increasing their temperature. This entails the necessity for an efficient volumetric heating system. More details about the design and optimization of the apparatus can be found in previous articles [32–34]. An intermediate vessel has been placed between the exit of the microwave cavity and the resin inlet into the vacuum bag. The vessel works as a buffer to decouple the heating system and the LCM apparatus to avoid a potential mismatch between the resin flow rate and the amount of energy provided by the microwaves [34], which could lead to an overheating of the catalyzed resin. The resin is driven through the microwave preheating cavity to the buffer vessel by positive pressure. The resin flow through the resonant cavity and the microwave power emitted have been calibrated by performing preliminary heating tests. A resin flow of 0.38l/min was set, while the power emitted by the magnetron was 2 kW.

3. Results and Discussion

Dielectric measurements and visual analysis of the flow front performed during the two tests are reported in Figures 5 and 6.

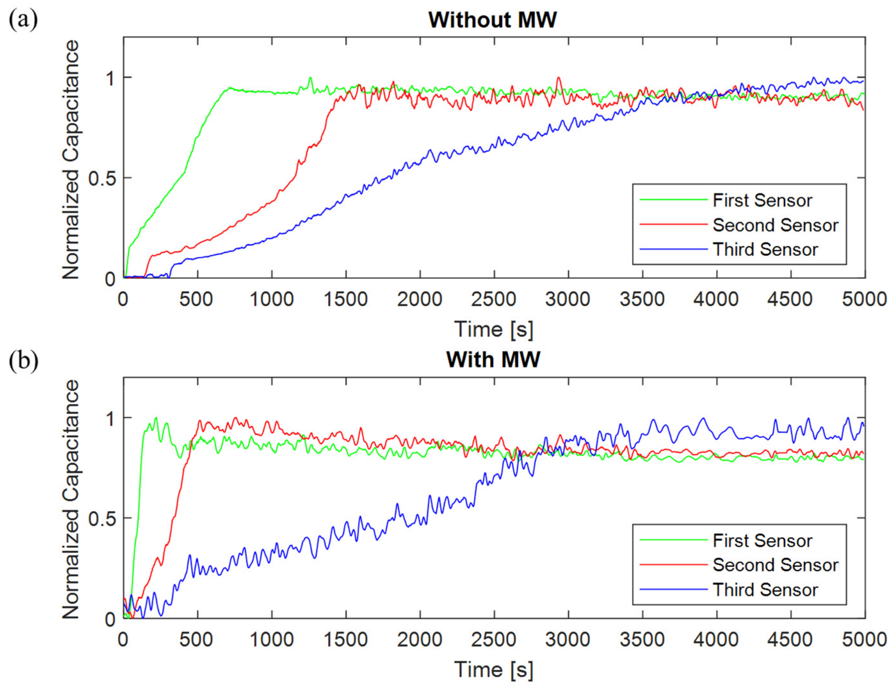

Figure 5. Dielectric acquisition in conventional resin infusion (**a**) and in resin infusion test with microwave preheating (**b**).

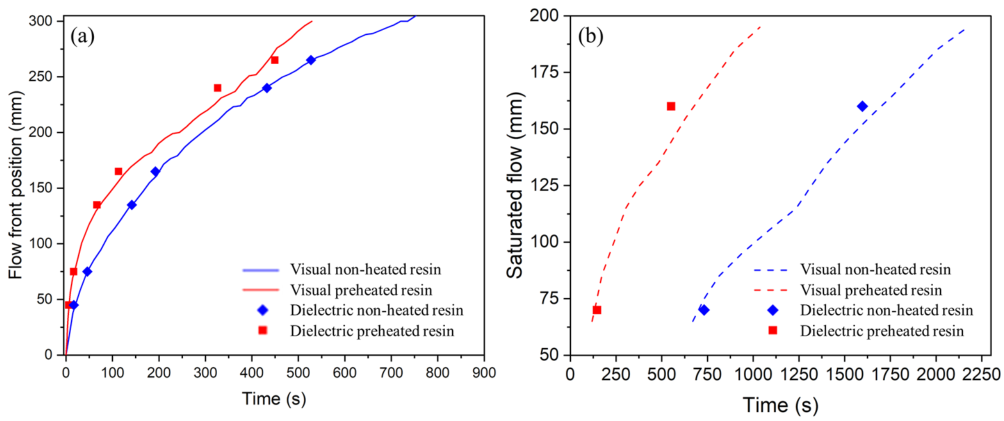

Figure 6. Visual resin flow front profiles compared with dielectric signals for resin arrival and preform saturation acquired during the two tests from top side (**a**) and bottom side (**b**).

The dielectric sensors detect variations in the capacitance of medium contained between the two armatures as the resin flow reach the sensor locations [19,20]. The observable variations in the signals during the infusion can be ascribed to the resin flow through the glass fiber fabric. Three distinct trends in the capacitance curves can be detected, which are more evident in the test without preheating where the resin flow is slower than that in the tests with resin preheating. The signal shows an initial increasing step, ranging from 8 to 15% of the saturated signal and is related to the flow of the resin through the flow media: the resin, indeed, promptly impregnated the distribution web covering almost immediately the sensing area due to its high permeability, which can be two orders of magnitude higher that the textile or even more. After that, the resin progressively fills the glass fabric layer below the flow media and the capacitance profile proceeds with a reduced slope until it reaches a plateau. At this point the proportion between resin and fibers stabilizes and the signal remains almost constant or without significant variations. Fluctuations of the signals are due to the continuous flow of the resin through the preform in the sensing areas. The capacitance curves of the three sensors present different slope for each phase of the infusion and are due to the reduction in the resin velocity as expected in case of applied constant gradient pressure, typical of the SCRIMP process. Therefore, the impregnation is faster at the beginning of the infusion and slows down as the infusion proceeds (it is also visible in the flow front profiles described in Figure 6)

By comparing the profiles of the signals from the two experiments, the effect of the preheating on the behavior of the resin is visible. The signal detected by sensor 1, located at 60 mm from the resin inlet, reaches the plateau with a remarkably advance when compared to the non-heated resin case (Figure 5). Despite that the first step related to the resin flow through the flow media, which does not show remarkable differences, the steeper curve describing the second stage of the infusion evidences how the impregnation of the glass fabric layers proceeds faster in the test with preheated resin reaching the saturation in approximately ten seconds after the arrival of the resin at the sensing location.

A similar trend can be observed at the locations of sensors 2 and 3, where saturation of the preform with preheated resin was achieved in less than half the time required by the non-heated resin. It is worthy of noting that the effect of the resin preheating cannot be appreciated at the very beginning of the infusion when resin first goes through the flow medium: the high permeability has a predominant effect on the resin velocity than the reduction in viscosity from the temperature increasing [36].

The advancement profiles of the resin flow front captured by the cameras during the two experiments are reported in Figure 6. The two profiles in Figure 6a refer to the resin advancing on the flow media, while Figure 6b shows the flow front of the resin acquired on the mold surface from the eyelet (Figure 2). The position of the flow front has been also acquired from the dielectric signals and reported in both graphs for the tests with unheated and preheated resin.

In both tests, the resin flow velocity decreases during the infusion. Indeed, the resin initially advances pushed by a high-pressure gradient and, during the infusion, the gradient decreases in relation to the advancement of the resin describing the conventional flow through a porous medium [36]. Figure 6 shows the difference between the two test cases. Indeed, the microwave preheated resin flow front reaches the vent in less than 70% of the non-heated resin. In the earliest 100 mm the microwave preheated resin flow front is more than twice faster if compared to the non-heated case: 2.3 mm/s for the preheated resin, 1.0 mm/s for the conventional process. The velocity difference decreases as the process continues. In the last 100 mm, the average flow front velocities are 0.34 mm/s and 0.23 mm/s, respectively.

The analysis of the flow-front detections acquired from the eyelets of the bottom half-mold indicate the complete impregnation of the preform, which is delayed with respect to the top flow due to the difference in the permeability of flow media and fiber fabric. Due to the design of the rigid half mold, the bottom flow front can be acquired only on the eyelet, which ranges from 65 to 195 mm from the inlet. Therefore, only data from sensors 1 and 2 can be correlated to the visual analysis, since the sensing area of sensor 3 is not covered by the eyelet. From data reported in Figure 6, it is possible to observe that while the reduction in filling time on the top of the preform is approximately 25% at 195 mm from the inlet, the difference in the bottom flow between the tests with preheating and non-heated resin is around 50%. Clearly, the flow through the distribution medium is less affected by the preheating, thanks to the high permeability of that medium (it is visible also in the dielectric signals, as mentioned before); on the other hand, it has a significant influence on the flow through the fabric where the reduction in the viscosity plays a major role in facilitating the impregnation of the fibers. The beneficial effect of microwave preheating, as reported in previous works [32–34], is related to the rheological behavior of thermoset resins: the temperature reached by the resin at the exit of the microwave cavity was approximately 36 °C, while the room temperature at which the test with non-heated resin was conducted was 22 °C; at 36 °C the viscosity decreases from 0.8 Pa·s up to 0.4 Pa·s, as shown in Figure 1. Nevertheless, the thermal energy conferred to the resin must be carefully tuned to avoid premature gelation of the thermoset. At the operative temperature reached by the resin in the test with preheating, no gelation occurred for the time required to complete the impregnation of the preform.

Table 3 summarizes the times of the resin flow when it reaches the sensing locations; the arrival on the sensor edges determining the first reaction of the sensors and the time when the resin reached the opposite edge and fully cover the sensor. The saturation time corresponds to the stabilization of the dielectric signals (Figure 5) and it represents the moment when the resin reaches the end of the sensing area on the bottom of the mold, and it has fully impregnated the whole thickness of the preform. The graphs in Figure 6 show the good agreement between the visual and dielectric analyses and the reliability of the latter in detecting the resin flow on both the top and the bottom of the mold.

Table 3. Times of resin flow arrival at sensing locations for tests with non-heated and preheated resin acquired by dielectric sensors and the saturation of the dielectric signals (in the parenthesis are reported the distances from the inlet port).

	Non-Heated Resin Infusion	**Preheated Resin Infusion**
	Time [s]	
Arrive to S1 (50 mm)	17.0	6.0
Arrive to end of S1 (70 mm)	46.0	16.5
Saturation S1	730	145
Arrive to S2 (140 mm)	140	66.5
Arrive to end of S2 (160 mm)	190	115
Saturation S2	1600	550
Arrive to S3 (230 mm)	415	325
Arrive to end of S3 (250 mm)	485	450
Saturation S3	5020	3810

By analyzing the dielectric data, it is possible to appreciate the benefits of the microwave heating method: a remarkable reduction in the infusion time in the test with microwave preheated resin was registered with the shortening of the saturation times of the three sensors by approximately 80%, 65%, and 30%, respectively. The top flow registered a smaller decrease in times of approximately 64 %, 52%, and 7%, respectively, on the three sensors.

Figures 7 and 8 depict a qualitative representation of the flow front derived from the data of the dielectric sensors at specific moments of the infusion.

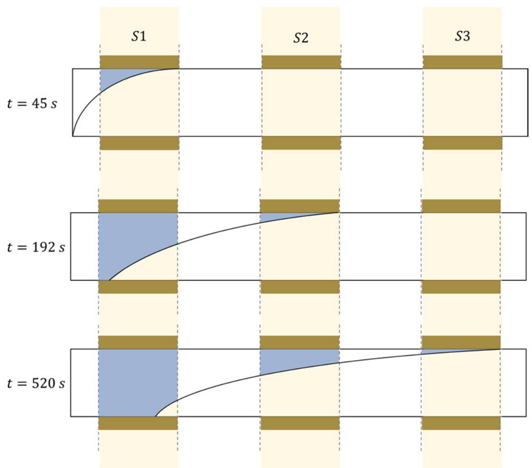

Figure 7. Schematic representation of flow front profile at the arrival of the resin on the sensing area for infusion with non-heated resin.

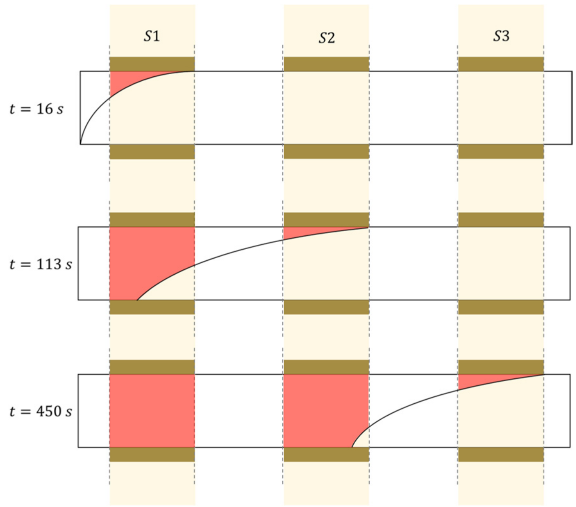

Figure 8. Schematic representation of flow front profile at the arrival of the resin on the sensing area for the infusion with microwave preheated resin.

In the SCRIMP process, the presence of a distribution medium determines the formation of two main flows: the first through the free-fibers region (i.e., the distribution medium) and the second through the fiber preform region (bulk porous medium). The former consists of a longitudinal flow from the inlet to the vent, while the second present a combination of a transverse flow (i.e., the out-of-plane flow through the thickness of the fiber preform) and a longitudinal one. This gives place to two regions characterized by different flow behaviors: a fully saturated zone, where the fluid flows through the preform with a velocity profile constant along the thickness of the preform, and a partially saturated zone, characterized by longitudinal and transverse flows through the thickness (Figure 8, time 450 s).

In the former region, the velocity vector is parallel to the main flow direction representing a fully developed flow, and meaning that the flow is substantially unidirectional with no significant crossed flows.

The flow in the latter zone is bi-directional (visual analysis indicated that in the in-plane flow no variations of the resin velocity occurred along the transversal direction) since the resin permeates from the distribution media in the through-the-thickness direction. The higher resin velocity along the longitudinal direction in the distribution medium determined a complex shape flow front. This feature characterizes the unsaturated region [36].

The formation of the unsaturated region, as mentioned before, occurred as the infusion begins due to the high longitudinal permeability of the distribution medium compared to the reinforcement one. In the unsaturated region, part of the liquid resin flows transversally from the distribution medium toward the preform, however, this transversal flow occurs to limited extent also in the saturated region determining the formation of a transition region between the saturated zone and flow front region [36].

Previous work by some of the authors [36] pointed out that the ratios between the thicknesses and between the permeabilities of the distribution medium and preform influence the extension of the unsaturated region and, hence, the delay between the first arrival of the resin to the vent and fully impregnation of the preform while other parameters, such as the fiber volume fraction or the compressibility of textiles, do not play a significant role. Therefore, in the present experimentation, the differences observed have to be ascribed to the change in rheological properties induced by the preheating being the other factors kept equal in the two tests.

In the infusion with non-heated resin, the unbalance in the permeability of distribution medium and fiber bulk determined a large difference in the resin velocity in the tow region resulting in a long unsaturated region (Figure 7). Indeed, when the resin reached the end of sensor 2 the preform in sensing area 1 is only partially filled, the signal is at 30% of its plateau and, by extension, it is possible assuming that the preform is impregnated by the same percentage. On the other hand, in the test with preheated resin the length of the unsaturated zone is far smaller and the preform in sensing area 1 is filled with the resin by almost 70%, consistently with the reduction in the time required by sensor 1 to reach the plateau in the two experiments (Table 3). Furthermore, it is possible to observe that when the resin reaches the end of sensor 3 the preform at sensor 1 location is still not fully impregnated: the resin reached that location almost 250 s in advance with respect to the saturation of the preform, which was approximately 77% (Table 3). The preform at the location of sensor 2, as consequence, result partially filled by only 17%. Conversely, in the test with preheating, the resin filled in a shorter time the preform thanks to the reduced viscosity and the enhanced flow resulting in a full impregnation at sensing area 1 and in a high level of saturation of the preform at the sensing area 2 of almost 80%. The analysis of the present preliminary experimentation indicates that microwave heating is effective to enhance the resin flow not only in the conventional RTM or VARTM processes [34] but also in the case of processes using a flexible half mold, such as SCRIMP, being able to further promote the impregnation and reduce the overall filling time more than that obtainable by using the sole distribution medium. The good agreement between dielectric signals and visual analysis also indicated the validity of the dielectric analysis and parallel-plate sensor for flexible-mold manufacturing processes. Further development involving the numerical analysis of the resin flow will be useful to strengthen the correlation between the actual position of the resin during the infusion and the signals from the dielectric sensors.

4. Conclusions

This paper compares the performances of the conventional resin infusion process and microwave preheated resin infusion in the case of flexible mold. The experiments conducted and the analysis of the achieved outcomes evidenced that the resin system preheating gives place to beneficial effects in the vacuum infusion processes, with a marked reduction in the cycle time. The reduction in the viscosity provokes an improvement of the flow, in agreement with Darcy's law. Considering the achieved results and what was discussed above, the following remarks can be drawn:

1. The unsaturated resin flow front is faster at the inlet due to the higher gradient of pressure. It decelerates during the infusion. In the present experiments, the final flow front velocity ranges between 15% and 22% of the initial velocity.
2. The flow front velocity is significantly affected by the microwave preheating: the resin reached vent 220 s earlier than in the non-heated resin case evidencing a reduction of 29% in the flow front crossing time.
3. The dielectric sensors detected a marked deceleration of the saturated resin flow as the distance from the resin inlet increased. The velocity decrease between sensor 1 (60 mm from the inlet) and sensor 3 (240 mm from the inlet) ranges between 84% and 92%.
4. The microwave preheating is beneficial to the infusion process. The dielectric measurement evidenced a decrease in overall saturation time of 50% correlated to a reduction in the length of the unsaturated region.

The presented results raise new interrogatives, such as the effects of microwave preheating on the fibrous preform saturation in vacuum bag infusion processes and resin system curing time, the effects related to the geometry and the architecture of the fibrous preform, or the influence of the binder applied, just to mention some of them. These aspects should be investigated by further analyses in future works.

Author Contributions: Conceptualization, F.R., F.T., V.E. and P.C.; methodology, F.R., F.T., V.E. and P.C.; formal analysis, F.R., F.T., V.E. and P.C.; investigation, F.R., F.T. and V.E.; resources, P.C.; data curation, F.R., F.T., V.E. and P.C.; writing—original draft preparation, F.R., F.T. and V.E.; writing—review and editing, F.R., F.T., V.E. and P.C.; visualization, F.R., F.T. and V.E.; supervision, P.C.; project

administration, P.C.; funding acquisition, P.C. All authors have read and agreed to the published version of the manuscript.

Funding: This research received no external funding.

Institutional Review Board Statement: Not applicable.

Informed Consent Statement: Not applicable.

Data Availability Statement: Not applicable.

Conflicts of Interest: The authors declare no conflict of interest.

References

1. Boutier, S.; Fourel, J.; Sanial, P. How To Make a Choice Between Liquid Composite Molding Processes? In Proceedings of the 9th International Conference on Flow Processes in Composite Materials-FPCM-9, Montréal, QC, Canada, 8–10 July 2008; pp. 1–8.
2. Roth, Y.C.; Weinholdt, M.; Winkelmann, L. Liquid Composite Moulding-Enabler for the Automated Production of CFRP Aircfraft Components. In Proceedings of the ECCM 16 - 16th European Conference on Composite Materials, Seville, Spain, 22–26 June 2014.
3. Park, C.H.; Woo, L. Modeling Void Formation and Unsaturated Flow in Liquid Composite Molding Processes: A Survey and Review. *J. Reinf. Plast. Compos.* **2011**, *30*, 957–977. [CrossRef]
4. Kuentzer, N.; Simacek, P.; Advani, S.G.; Walsh, S. Correlation of Void Distribution to VARTM Manufacturing Techniques. *Compos. Part A Appl. Sci. Manuf.* **2007**, *38*, 802–813. [CrossRef]
5. Hamidi, Y.K.; Altan, M.C. Process Induced Defects in Liquid Molding Processes of Composites. *Int. Polym. Process.* **2017**, *32*, 527–544. [CrossRef]
6. Terekhov, I.V.; Chistyakov, E.M. Binders Used for the Manufacturing of Composite Materials by Liquid Composite Molding. *Polymers* **2022**, *14*, 87. [CrossRef] [PubMed]
7. Molimard, J.; Vacher, S.; Vautrin, A. Monitoring LCM Process by FBG Sensor Under Birefringence. *Strain* **2011**, *47*, 364–373. [CrossRef]
8. Gupta, N.; Sundaram, R. Fiber Optic Sensors for Monitoring Flow in Vacuum Enhanced Resin Infusion Technology (VERITy) Process. *Compos. Part A Appl. Sci. Manuf.* **2009**, *40*, 1065–1070. [CrossRef]
9. Tucci, F.; Rubino, F.; Carlone, P. Strain and Temperature Measurement in Pultrusion Processes by Fiber Bragg Grating Sensors. *AIP Conf. Proc.* **2018**, *1960*, 020036. [CrossRef]
10. Di Fratta, C.; Klunker, F.; Ermanni, P. A Methodology for Flow-Front Estimation in LCM Processes Based on Pressure Sensors. *Compos. Part A. Appl. Sci. Manuf.* **2013**, *47*, 1–11. [CrossRef]
11. Tuncol, G.; Danisman, M.; Kaynar, A.; Sozer, E.M. Constraints on Monitoring Resin Flow in the Resin Transfer Molding (RTM) Process by Using Thermocouple Sensors. *Compos. Part A. Appl. Sci. Manuf.* **2007**, *38*, 1363–1386. [CrossRef]
12. Tucci, F.; Bezerra, R.; Rubino, F.; Carlone, P. Multiphase Flow Simulation in Injection Pultrusion with Variable Properties. *Mater. Manuf. Process.* **2020**, *35*, 152–162. [CrossRef]
13. Vedernikov, A.; Safonov, A.; Tucci, F.; Carlone, P.; Akhatov, I. Modeling Spring-In of L-Shaped Structural Profiles Pultruded at Different Pulling Speeds. *Polymers* **2021**, *13*, 2748. [CrossRef] [PubMed]
14. Vedernikov, A.; Tucci, F.; Safonov, A.; Carlone, P.; Gusev, S.; Akhatov, I. Investigation on the Shape Distortions of Pultruded Profiles at Different Pulling Speed. *Procedia Manuf.* **2020**, *47*, 1–5. [CrossRef]
15. Dominauskas, A.; Heider, D.; Gillespie, J.W. Electric Time-Domain Reflectometry Sensor for Online Flow Sensing in Liquid Composite Molding Processing. *Compos. Part A Appl. Sci. Manuf.* **2003**, *34*, 67–74. [CrossRef]
16. Vaidya, U.K.; Jadhav, N.C.; Hosur, M.V.; Gillespie, J.W.; Fink, B.K. Assessment of Flow and Cure Monitoring Using Direct Current and Alternating Current Sensing in Vacuum-Assisted Resin Transfer Molding. *Smart Mater. Struct.* **2000**, *9*, 727–736. [CrossRef]
17. Hancioglu, M.; Sozer, E.M.; Advani, S.G. Comparison of In-Plane Resin Transfer Molding and Vacuum-Assisted Resin Transfer Molding 'Effective' Permeabilities Based on Mold Filling Experiments and Simulations. *J. Reinf. Plast. Compos.* **2020**, *39*, 31–44. [CrossRef]
18. Tifkitsis, K.I.; Skordos, A.A. A Novel Dielectric Sensor for Process Monitoring of Carbon Fibre Composites Manufacture. *Compos. Part A Appl. Sci. Manuf.* **2019**, *123*, 180–189. [CrossRef]
19. Carlone, P.; Rubino, F.; Paradiso, V.; Tucci, F. Multi-S.Scale Modeling and Online Monitoring of Resin Flow through Dual-Scale Textiles in Liquid Composite Molding Processes. *Int. J. Adv. Manuf. Technol.* **2018**, *96*, 2215–2230. [CrossRef]
20. Carlone, P.; Palazzo, G.S. Unsaturated and Saturated Flow Front Tracking in Liquid Composite Molding Processes Using Dielectric Sensors. *Appl. Compos. Mater.* **2015**, *22*, 543–557. [CrossRef]
21. Lee, H.L. *The Handbook of Dielectric Analysis and Cure Monitoring*, 2nd ed.; Lambient Technologies LLC: Cambridge, MA, USA, 2014.
22. Qing, X.; Liu, X.; Zhu, J.; Wang, Y. In-Situ Monitoring of Liquid Composite Molding Process Using Piezoelectric Sensor Network. *Struct. Health Monit.* **2020**. [CrossRef]

23. Abraham, D.; Mcilhagger, R. Glass Fibre Epoxy Composite Cure Monitoring Using Parallel Plate Dielectric Analysis in Comparison with Thermal and Mechanical Testing Techniques. *Compos. Part A. Appl. Sci. Manuf.* **1998**, *29*, 811–819. [CrossRef]
24. Hegg, M.C.; Ogale, A.; Mescher, A.; Mamishev, A.V.; Minaie, B. Remote Monitoring of Resin Transfer Molding Processes by Distributed Dielectric Sensors. *J. Compos. Mater.* **2005**, *39*, 1519–1539. [CrossRef]
25. McIlhagger, A.; Brown, D.; Hill, B. Development of a Dielectric System for the On-Line Cure Monitoring of the Resin Transfer Moulding Process. *Compos. Part A Appl. Sci. Manuf.* **2000**, *31*, 1373–1381. [CrossRef]
26. Kim, H.G.; Lee, D.G. Dielectric Cure Monitoring for Glass/Polyester Prepreg Composites. *Compos. Struct.* **2002**, *57*, 91–99. [CrossRef]
27. Rubino, F.; Nisticò, A.; Tucci, F.; Carlone, P. Marine Application of Fiber Reinforced Composites: A Review. *J. Mar. Sci. Eng.* **2020**, *8*, 26. [CrossRef]
28. Zhang, K.; Gu, Y.; Wang, S.; Li, M.; Zhang, Z. Effects of Preheating Temperature of the Mould on the Properties of Rapid-Curing Carbon Fibre Composites Fabricated by Vacuum-Assisted Resin Infusion Moulding. *Polym. Polym. Compos.* **2014**, *22*, 825–836. [CrossRef]
29. Zhang, K.M.; Gu, Y.Z.; Li, M.; Wang, S.K.; Zhang, Z.G. Resistive Heating of Carbon Fiber Aided Rapid Curing of Vacuum Assisted Resin Infusion Molding. *Adv. Mater. Res.* **2014**, *1030–1032*, 170–173. [CrossRef]
30. Johnson, M.S.; Rudd, C.D.; Hill, D.J. The Effect of Microwave Resin Preheating on the Quality of Laminates Produced by Resin Transfer Molding. *Polym. Compos.* **1997**, *18*, 185–197. [CrossRef]
31. Rudd, C.D.; Kendall, K.N. Towards a Manufacturing Technology for High-Volume Production of Composite Components. *Proc. Inst. Mech. Eng. Part B J. Eng. Manuf.* **1992**, *206*, 77–91. [CrossRef]
32. Esperto, V.; Durante, M.; Carlone, P.; Carrino, L. Resin Microwave Preheating in Liquid Composite Molding Process. *AIP Conf. Proc.* **2019**, *2113*, 110007. [CrossRef]
33. Rubino, F.; Paradiso, V.; Carlone, P. Flow Monitoring of Microwave Pre-Heated Resin in LCM Processes. *AIP Conf. Proc.* **2017**, *1896*, 030017. [CrossRef]
34. Rubino, F.; Esperto, V.; Tucci, F.; Carlone, P. Flow Enhancement in Liquid Composite Molding Processes by Online Microwave Resin Preheating. *Polym. Eng. Sci.* **2020**, *60*, 2377–2389. [CrossRef]
35. Esperto, V.; Boccarusso, L.; Durante, M.; Carrino, L.; Carlone, P. Permeability Analysis of Natural and Artificial Fiber Textiles for Liquid Composite Molding Process. *Procedia Manuf.* **2020**, *47*, 435–439. [CrossRef]
36. Rubino, F.; Carlone, P. A Semi-Analytical Model to Predict Infusion Time and Reinforcement Thickness in VARTM and SCRIMP Processes. *Polymers* **2019**, *11*, 20. [CrossRef] [PubMed]